

# Magneto-Compound Reaction of Convective Flow via a Porous Inclined Plate with Heat Energy Absorption

D. Chenna Kesavaiah<sup>1</sup>, B Venkateswarlu<sup>2,†</sup>, N. Nagendra<sup>3</sup> and O.D.  
Makinde<sup>4</sup>

**Abstract** The current study is concerned with the unsteady heat and mass transfer of MHD free convection flow via a porous inclined plate that accelerates exponentially with temperature and concentration. Heat emission, source/sink, radiation absorption, and reaction are taken into account in the energy and species equations. The innovative part of the work is the analysis of the flow phenomenon with a heat source or sink and radiation absorption along the chemical reaction. The governing PDEs are reduced into ODEs via the non-dimensional variables and afterward solved analytically utilizing the perturbation strategy. Graphical representations of liquid temperature, speed, and concentration as well as the Sherwood & Nusselt quantities and the skin friction factor are displayed in tabular form for different combinations of appropriate stream quantities. The analysis of a resistance quantum grows with the size of the magnetic, whereas the rates of mass and heat transfer decline with increasing radiation, reaction, and Schmidt number. Thermal-velocity and concentration-velocity profiles interact reciprocally with the accelerating radiation, heat source, and compound reaction. The growth of speed and thermal profiles is clearly visible due to the absorption and Prandtl values. The present results are in strongly consistent with the earlier published results. There are numerous applications for this research in many sectors and material processing for understanding drag in seepage flows on heated/cooled and inclined surfaces.

**Keywords** Convection Flow, MHD, porous medium, chemical reaction, inclined plate, radiation

**MSC(2010)** 76W05, 76E06, 76S05, 80A32.

## 1. Introduction

One of the most intriguing research topics over the past 200 years has been on the phenomenon of convection flows in porous media. This fascination is a result of

---

<sup>†</sup>the corresponding author.

Email address: [bvenkateswarlu.maths@gmail.com](mailto:bvenkateswarlu.maths@gmail.com)

<sup>1</sup>Department of BS and H, Vignan Institute of Technology and Science, Deshmukhi-508284, T.S., India. [chennakesavaiah@gmail.com](mailto:chennakesavaiah@gmail.com)

<sup>2</sup>School of Mechanical Engineering, Yeungnam University, Gyeongas-n-38541, Republic of Korea. [bvenkateswarlu.maths@gmail.com](mailto:bvenkateswarlu.maths@gmail.com)

<sup>3</sup>Department of Mathematics, Sree Sai Institute of Technology and Science, Rayachoty-516270, A.P., India. [nagmaths@gmail.com](mailto:nagmaths@gmail.com)

<sup>4</sup>Faculty of Military Science, Stellenbosch University, Stellenbosch 7602, South Africa. [makinded@gmail.com](mailto:makinded@gmail.com)

its wide range of uses, which include electronic cooling, geothermal and building filtration systems, metallurgy, oceanography, chemical industries, etc. Husain et al. [1] and Siddartha et al. [2] reviewed the various applications (e.g. the design of atomic reactor, ventilation in building, aircraft cabin protection, electronic gear cooling, warming control, etc.) on the warm execution of natural convective flow through vertical annulus. A report on natural convective flow via an inclined plate was published by Roy et al. [3]. Abderrahmane et al. [4] scrutinized the convective flow of nanofluid due to a porous tending annulus by using a finite element technique. Convective flow of nanofluid via porous inclined wavy cavity was published by Ahmed [5], who concluded that it is more compelling for the rate of heat transmission compared to the restricting case. Khan et al. [6] examined the convective elements of pressing steam due to slanted rheology by using a homotopic system and found that the Ohmic warming and dissipation are utilized to upgrade the heat move. The convection flow towards an inclined channel plate was inspected by Kumar and Chandran [7]. Yang et al. [8] demonstrated the Laplace and Fourier sine transforms for convective steam of bio-nanofluid and found that the nanofluid speed diminished with upgrading of the second-grade liquid boundary.

The research in MHD steam of electrically conductive liquid is really of incredible importance because the magnetic field impacts on the boundary layer stream regulation control along with the adequacy of various frameworks utilizing electrically conductive fluids and their application in many engineering problems. For example, industrial machinery like pumps, bearings, generators of MHD, boundary control, etc., are impacted by the interaction of an electrically conducting fluid. Zafar et al. [9] projected the convective stream on an inclined plate through a magnetic field. They predicted that the magnetic field strength would be controlled by the fluid motion and also the magnetic field inclination point. The unsteady 2D convective flow of magnetic nanofluid was examined by Geridomez and Oztop [10]. They concluded that convective hotness increases with one-sided radiator length, volume fraction, and Rayleigh number, but decreases with an increase in Lorentz power. Ali et al. [11] demonstrated the magneto convective nanofluid flow in a rotating system filled with cavities by FEM and noticed that the magnetic field strength constricts the smooth movement and heat transfer rate extensively. Roy [12] obtained the solutions for the convective flow of a hybrid nanofluid via rectangular enclosure by FDM. He found that the stream function is reciprocal with the magnetic field and Rayleigh number, but the streamlines are in symmetry when the magnetic field angle is zero and  $\pi/2$ . Researchers [13]- [22] have been examining the various features of the convective flow of Williamson nanofluid together with a magnetic field.

Thermal radiation is used in many areas, such as agriculture (i.e., to improve food production and packaging), archaeology, space exploration, law enforcement, geology, etc. For example, by removing toxic pollutants (i.e., exacting gases from industry and coal-terminated power stations), electron beam radiation can remove dangerous  $NO_2$  and  $SO_2$  from our environment. In addition, the large number of textures cases our attire to have been lighted (i.e., treated by energy) prior to being presented to a dirt delivering or wrinkle-safe, compound and tissue therapy makes the chemicals bind to the fabric so that it keeps our fresh clothing and wrinkle-free all day. The authors [23], [24] published the heat charge impact on magneto-radiative nano & hybrid nanofluids via a porous elastic sheet. The study is used in medical fields (i.e. drug delivery, cancer therapy, etc.), magnetic power production processes, etc. Radiative Sakiadis flow via a tending plate was examined by Abbas

et al. [25]. They determined that the behaviour of temperature is reciprocal to velocity with the magnetic field, density variation, and heat emission. Roy et al. [26] published the EHD (i.e., electrohydrodynamics) convective flow due to a circular cylinder in radiation and they directed the heat transfer at the cylinder (i.e. inner & outer). This affirms that radiation is the prevailing way of heat up convey. Rani et al. [27] implemented the Laplace transform technique on the convective stream caused by a permeable inclined plate due to radiative viscous fluid and magnetic field. The radiative Oldroyd-B nanofluid flow in an axisymmetric rotating disk was demonstrated by Khan et al. [28] and Hafeez et al. [29]. Their investigation revealed that the presence of radiative heat flux effectively improves the thermal profile.

The chemical response is a reversible or irreversible interaction in which two distinct kinds of synthetic constituents respond to frame a solitary item within the sight of a protein or impetus. There has been a heightened interest in the advancement of synthetic cycles, prompting energy reserve funds or improving their proficiency. Also, the synthetic response plays a crucial role in handling modest unrefined substances into high-value items in the compound handling ventures. Hence, this peculiarity plays a critical part in the substantial business, power, and cooling industries for drying, vanishing, energy moving in the stream in a desert cooler, etc. Swain [30] imposed the Crank-Nicolson scheme for the MHD convective flow of viscous fluid via a porous vertical plate with chemical reaction. The important research results show that the reaction parameter decreases velocity while the heat source increases it. The industries and systems utilized to process materials were the main focus of this investigation. The effects of chemical reactions on Cattaneo-Christove flow of Oldroyd-B nanofluid flow were studied by Hafeez and Khan [31] and Hafeez et al. [32, 33]. The chemical response and Hall impacts on magnetic transient/micropolar fluid flow were examined by Raju et al. [34], Sing et al. [35], Satya Narayana et al. [36, 37] and Das [38]. This study is used in research fields like biomedical, aerodynamics, geothermal systems, heat exchangers, ground water pollution, etc. Qiang et al. [39] obtained analytical solutions for 2D convective flow of an inclined magnetic field between two unbounded vertical plates with chemical reaction. Chemically reacting MHD convective flow due to an inclined surface was explored by Ahmad et al. [40] and they found that the fluid flow velocity was enlarged by thermal thickness and conductivity. Heat transfer analysis of scutter by liquid through chemical reaction impacts was theoretically exposed by Imran et al. [41].

It is noticed that there is an extensive hotness distinction between the liquid and the surface layer of the solid body in numerous liquid problems of practical interest. In the current investigation, we have considered the unsteady 2D hydromagnetic natural convection stream in a rapidly inclined hastened under the influence of heat emission, generation, absorption and chemical reaction. The governing PDEs are reduced into ODEs via the non-dimensional variables and then solved analytically using the perturbation procedure. Graphical representations of numerical values of liquid concentration, speed, hotness profiles among the friction factor, heat and mass transmission rates are displayed in the tabular form for dissimilar pertinent stream quantities.

## 2. Problem formulation

Consider a 2D unsteady convective flow of magnetohydrodynamically thick, incompressible, and radiation absorption liquid caused by a porous, dramatically accelerated, and slanted endless plate. Fig.1 represents the physical model and the axes  $x', y'$  are correspondingly engaged through and normal to the plate. The magnetic field strength  $B_0$  is applied to the path at right angles to the plate.  $\gamma$  is the angle to which the plate is inclined in the vertical direction. The magnetic Reynolds steam is extremely small. As a result we can neglect the induced magnetic field. First, we assume  $T'_\infty$  temperature and  $C'_\infty$  concentrations which are the same for the plate and the surrounding fluid. In the plane where the plate is placed, we exponentially accelerate the plate at  $t'$  with a speed of  $u' = u_0 e^{a't'}$ . The concentration and hotness stage are increased or decreased linearly with respect to time  $t$ .

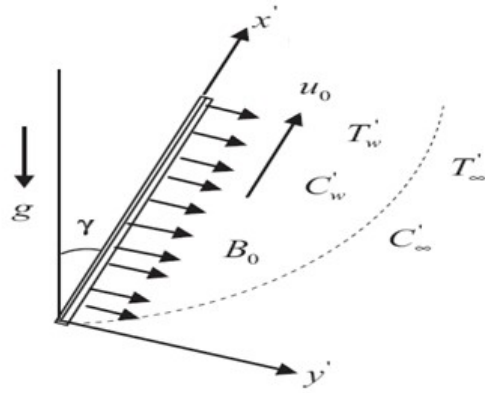


Figure 1. Physical model and flow geometry

The steam administering conditions (see Ref. [27] & [42]) can be composed as

$$\left( \frac{\partial^2}{\partial y'^2} - \frac{\partial}{\partial t'} - \frac{\sigma B_0^2}{\rho} - \frac{\nu}{K'_p} \right) (u') + g \{ \beta (T' - T'_\infty) + \beta' (C' - C'_\infty) \} \cos \gamma = 0, \quad (2.1)$$

$$\left( k \frac{\partial^2}{\partial y'^2} - \rho C_p \frac{\partial}{\partial t'} \right) (T') - \frac{\partial}{\partial y'} (q_r) + Q' (T' - T'_\infty) + Q' (C' - C'_\infty) = 0, \quad (2.2)$$

$$\left( D \frac{\partial^2}{\partial y'^2} - \frac{\partial}{\partial t'} \right) (C') - K'_r (C' - C'_\infty) = 0. \quad (2.3)$$

The preliminary and border line settings are provided by

$$\begin{aligned} C' &= C'_\infty, T' = T'_\infty, u' = 0, & : y', t' \leq 0 \\ \nu(C' - C'_\infty) &= t' u_0^2 (C'_w - C'_\infty), \nu(T' - T'_\infty) = t' u_0^2 (T'_w - T'_\infty), \\ u' - u_0 e^{a't'} &= 0, & : y' = 0, t' > 0 \\ C' - C'_\infty &\rightarrow 0, T' - T'_\infty \rightarrow 0, u' \rightarrow 0 \end{aligned} \quad (2.4)$$

The fluid, assumed as grey, discharging/retaining radiation, however, is a non-dispersing medium, and hence the gradient expression for the instance of an optically thin grey gas (see Ref. [43, 44]) is given by

$$4a^* \sigma (T_\infty'^4 - T'^4) + \frac{\partial q_r}{\partial y} = 0. \quad (2.5)$$

We can express  $T'^4$  as a direct capacity of temperature since the temperature difference within the stream is sufficiently minimal. To do this, we expand  $T'^4$  in a Taylor series about  $T_\infty'$  and, ignoring the higher order terms, we obtain

$$T'^4 \cong 4T_\infty'^3 T' - 3T_\infty'^4. \quad (2.6)$$

Using equations (2.5) and (2.6). we have

$$\left( k \frac{\partial^2}{\partial y'^2} - \rho C_p \frac{\partial}{\partial t'} \right) (T') - \frac{\partial}{\partial y'} (q_r) - 16a^* \sigma T_\infty'^3 (T' - T_\infty') + Q'(C' - C'_\infty) = 0. \quad (2.7)$$

The following non-dimensional quantities are introduced (see Ref. [27]).

$$\begin{aligned} u_0 y' &= \nu y, u_0 U = u', \nu t = t' u_0^2 a' \nu, T(T'_w - T'_\infty) = T' - T'_\infty \\ C(C'_w - C'_\infty) &= (C' - C'_\infty), K = \frac{u_0^2 K'_p}{\nu^2}, Kr = \frac{Kr' \nu}{u_0^2}, Q = \frac{\nu Q'}{\rho C_p u_0^2}, \\ Sc &= \frac{\nu}{D}, M = \frac{\sigma B_0^2 \nu}{\rho u_0^2}, R = \frac{16a^* \nu^2 \sigma T'_\infty}{k u_0^2}, Pr = \frac{\mu C_p}{k}, \\ Gr &= \frac{\nu \beta g (T'_w - T'_\infty)}{u_0^3}, Gc = \frac{\nu \beta g (C'_w - C'_\infty)}{u_0^3}, Q_l = \frac{Q'_l \nu^2 (C'_w - C'_\infty)}{\rho C_p u_0^2 (T'_w - T'_\infty)}. \end{aligned} \quad (2.8)$$

With the help of equation (2.8), the equations (2.1)–(2.3) & (2.4) will rise to

$$\frac{\partial U}{\partial t} = \frac{\partial^2 U}{\partial y^2} - \left( M + \frac{1}{k} \right) U + GrT + Gc \cos \gamma, \quad (2.9)$$

$$\frac{\partial T}{\partial t} = \frac{1}{Pr} \frac{\partial^2 T}{\partial y^2} - \left( \frac{R}{Pr} + Q \right) T + Q_l C, \quad (2.10)$$

$$\frac{\partial C}{\partial t} = \frac{1}{Sc} \frac{\partial^2 C}{\partial y^2} - KrC. \quad (2.11)$$

The dimensionless form of initial and BCs is

$$\begin{aligned} C = T = U &= 0, & : y, t \leq 0, \\ C = T = t, U &= \exp(at) = 0 : y = 0, t > 0, \\ C, T, U &\rightarrow 0, u \rightarrow 0 : y \rightarrow \infty, t > 0. \end{aligned} \quad (2.12)$$

### 3. Solution to the problem

Equations (2.9)–(2.11) are coupled and non-linear PDEs that cannot be solved in any closed form using the primary and margin conditions (2.12). In any case, these conditions can be changed into a group of ODEs, which can be addressed methodically by utilizing the perturbation scheme. To accomplish this, we address the concentration, temperature, and speed of the liquid in the region of the plate as

$$\begin{aligned} U &= \varepsilon U_1(y)e^{at} + U_0(y), \\ T &= \varepsilon T_1(y)e^{at} + T_0(y), \\ C &= \varepsilon C_1(y)e^{at} + C_0(y). \end{aligned} \quad (3.1)$$

Replacing of condition (3.1) in equations (2.9)–(2.11) and comparing the terms of harmonic and non-harmonic will ascend to

$$U_0'' - \beta_4 U_0 = -GrT_0 \cos\gamma - GcC_0 \cos\gamma, \quad (3.2)$$

$$U_1'' - \beta_4 U_1 = -GrT_1 \cos\gamma - GcC_1 \cos\gamma, \quad (3.3)$$

$$T_0'' - (R + QPr)T_0 = -QPrC_0, \quad (3.4)$$

$$T_1'' - \beta_2 T_1 = -Q_i Pr C_1, \quad (3.5)$$

$$C_0'' - ScKrC_0 = 0, \quad (3.6)$$

$$C_1'' - \beta C_1 = 0. \quad (3.7)$$

As a result, the border situations can be composed as follows

$$\begin{aligned} \text{At } y = 0 : C_0 = T_0 = 1, U_0 = 0, \\ \& \quad C_1 = T_1 = 0, U_1 = 1, \end{aligned} \quad (3.8)$$

$$\text{As } y \rightarrow \infty : C_0 = T_0 = U_0 \rightarrow 0 \text{ and } C_1 = T_1 = U_1 \rightarrow 0.$$

Solving equations (3.2) to (3.7), along with border line situations (3.8), we obtain the following solutions:

$$C_0 = e^{m_1 y}, \quad (3.9)$$

$$C_1 = 0, \quad (3.10)$$

$$T_0 = A_1 e^{m_1 y} + A_2 e^{m_2 y}, \quad (3.11)$$

$$T_1 = 0, \quad (3.12)$$

$$U_0 = L_1 e^{m_2 y} + L_2 e^{m_1 y} + L_3 e^{m_3 y}, \quad (3.13)$$

$$U_1 = 0. \quad (3.14)$$

In view of equations (3.9) to (3.14), equation (3.1) becomes

$$U = L_1 e^{m_2 y} + L_2 e^{m_1 y} + L_3 e^{m_3 y}, \quad (3.15)$$

$$T = A_1 e^{m_1 y} + A_2 e^{m_2 y}, \quad (3.16)$$

$$C = e^{m_1 y}. \quad (3.17)$$

## 4. Physical engineering interest

The skin-friction factor and the mass and heat transform rates are given by

$$C_f = \left( \frac{\partial U}{\partial y} \right)_{y=0} = m_2 L_1 + m_1 L_2 + m_3 L_3, \quad (4.1)$$

$$Nu = \left( \frac{\partial T}{\partial y} \right)_{y=0} = A_1 m_1 + A_2 m_2, \quad (4.2)$$

$$Sh = \left( \frac{\partial C}{\partial y} \right)_{y=0} = m_1. \quad (4.3)$$

## 5. Results and discussions

The solution to altered ODEs with correlated boundary conditions was acquired with the aid of the perturbation technique. The impact of some existing objective quantities  $Gr$ ,  $Gc$ ,  $K$ ,  $Kr$ ,  $M$ ,  $Pr$ ,  $R$ ,  $Q$ ,  $Q_l$  and  $Sc$  on liquid speed, hotness and concentration is elucidated in Figs.2-12 and Tables 1– 3. In order to validate the exactness of our outcomes, Table 1 compares the present findings with the earlier published results of Rani et al. [27] and finds that the current results are in strong agreement with the earlier findings. From the study of Table 1 with the values of  $Gr = 10$ ,  $Gc = 5$ ,  $K = 0.5$ ,  $Kr = 0.2$ ,  $t = 0.4$ ,  $Pr = 0.71$ ,  $R = 1.0$ ,  $Sc = 0.6$ ,  $\gamma = \pi/6$ ,  $a = 0.5$ ,  $Q = 2.0$  and  $Q_l = 0$ , it is concluded that, the shear stress ( $C_f$ ) up-grades with the strong support of magnetic field. According to Tables 2 & 3, the mass transfer ( $Sh$ ) and the heat transfer rate ( $Nu$ ) rates both decline as the parameters  $R$  and  $Kr$  rise.

Fig. 2 plots the impact of Grashof and modified Grashof numbers on the liquid speed. It is seen that, on the expanding upsides of  $Gr$  &  $Gc$ , the increment of speed quickly approaches to the permeable plate and afterward rots flawlessly to the free stream speed. In addition, there is an ascent in the speed because of the enhancement of buoyancy force. This truly implies that, the buoyancy forces improve liquid speed and intensify the limit layer thickness with expansion of Grashof number and modified Grashof numbers.

Fig.3 outlines the variety of speed profiles across the limit layer for different levels of permeability and magnetic field parameters. In this figure, it is noticed that, an expansion of  $M$  leads to a decline in the fluid speed while the liquid speed increases with an expanding value of  $K$ . In this way, an electrically directed liquid rising to a Lorentz force has tended to slow down the fluid motion and both the

magnetic field produced the particle and its velocity are vertical direction to the Lorentz force. Furthermore, the permeability controls the movement of directional and the repository liquid flow rate in the formation.

Figs.4(a) and (b) show how the chemical reaction quantity affects liquid concentration and speed. The liquid velocity heightens in the higher reaction rate, though the contrary is marked in the concentration. Physically, the higher the chemical reaction, the lower the atomic diffusivity and the greater the species transfer acquired. In this manner, the concentration diminishes at all points of the steam field through an increase of  $Kr$ , and hence the rates of dispersion can be massively adjusted by the compound reaction.

Fig.5 is plotted for various upsides of the Prandtl number against the liquid hotness and speed. The speed  $U$  and hotness  $T$  show an expanding nature via an increase in  $Pr$ . The higher Prandtl number shows the lower thermal diffusivity and various types of liquids contain the lower warm diffusivity, which addresses the decrement in temperature. In addition, the thickness of the limit layer lies on boundary layer thickness depending on the Prandtl amount (i.e.,  $Pr > 1$  or  $Pr = 1$  or  $Pr < 1$ ) and if  $Pr = 1$ , it implies that the thickness of the warm limit layer is equivalent to that of the speed limit layer. The reason is that heat is able to diffuse away from the heated plate more quickly for higher values of  $Pr$  because smaller values of  $Pr$  are comparable to an increase in the thermal conductivity.

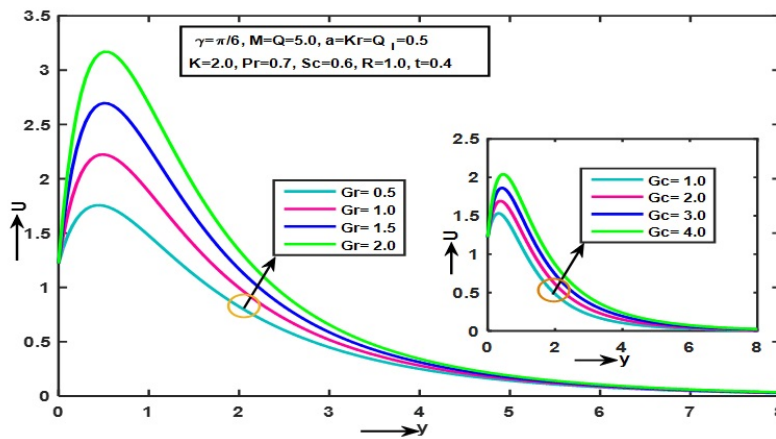


Figure 2.  $Gr$  &  $Gc$  impact on  $U$ .

The impact of variations in radiation quantity on the liquid hotness and speed distributions is illustrated in Fig.6. It is seen that when  $R$  accelerates, the fluid speed reduces. In addition, the extent of the stream wise speed diminishes and the emphasis point for the speed creates some distance from the plate. It is elevated in the radiation that conveys more hotness to the liquid, which prompts a frivolity in the liquid hotness. Thus, the emission is utilized where the higher heat distraction is essential, for instance, atomic reactors, polymers, glass, etc. Additionally, it has been observed that the boundary layer always gets thicker in the presence of



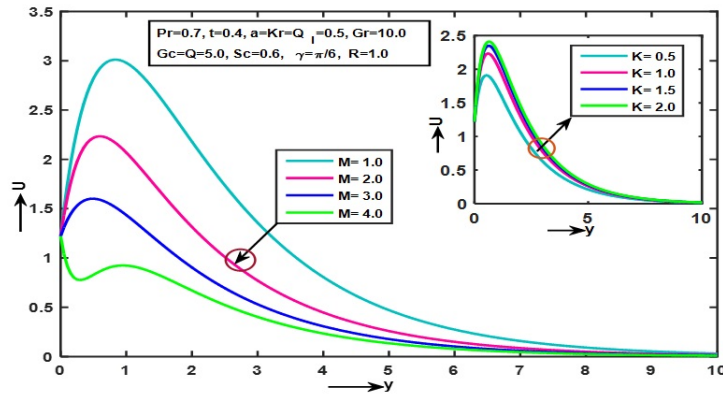


Figure 3.  $M$  &  $K$  impact on  $U$ .

Table 1.  $C_f$  Comparability

M	Rani et al. [27]	Present Study
0.0	0.9254	0.6909
1.0	1.2387	0.7814
5.0	2.3617	0.8763

Table 2.  $C_f$  Comparability

$R$	$Pr$	$Q$	$Q_l$	$Kr$	$Sc$	$t$	$Nu$
0.5	0.71	2.0	0.5	0.5	0.6	0.2	0.2869
1.0	0.71	2.0	0.5	0.5	0.6	0.2	0.2433
1.5	0.71	2.0	0.5	0.5	0.6	0.2	0.2166
2.0	0.71	2.0	0.5	0.5	0.6	0.2	0.1977

Table 3.  $Sh$  Variations

$Kr$	$Sc$	$t$	$Sh$
0.2	0.6	0.4	1.2688
0.2	1.0	0.4	0.5674
0.5	0.6	0.4	0.8228
1.0	0.6	0.4	0.5750

radiation, which may be justified given that radiation offers an extra pathway for energy diffusion.

Fig.7 is plotted for different principles of heat source limitation ( $Q$ ) against the hotness and speed. It is clear that the speed raises and the temperature diminishes

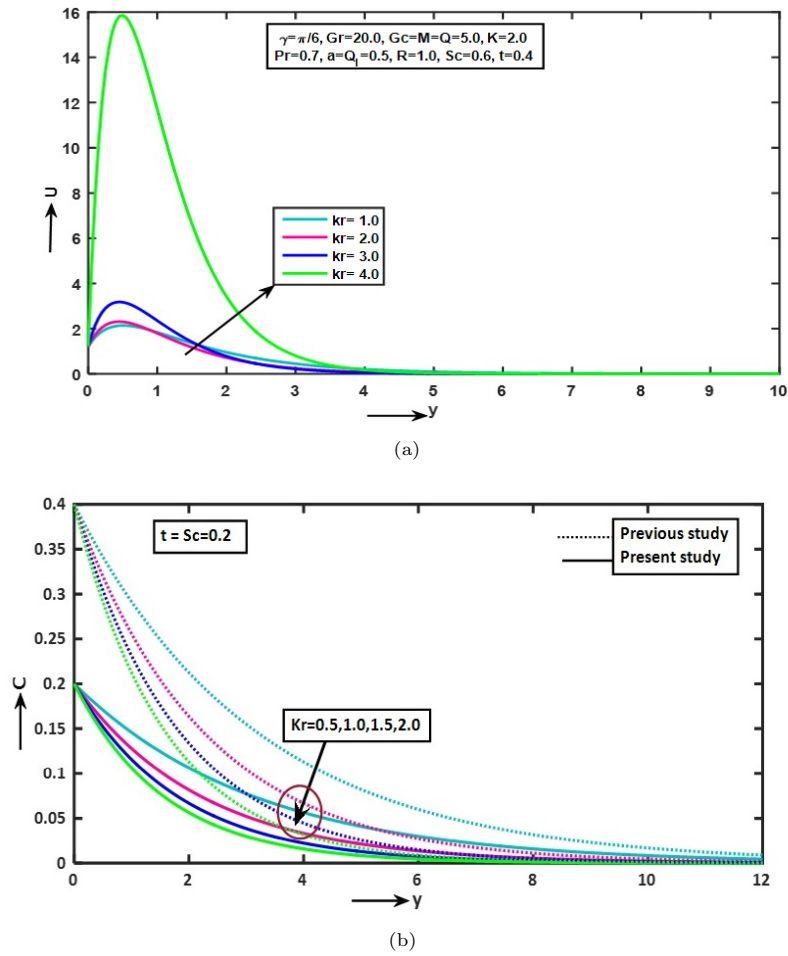


Figure 4.  $Kr$  impact on (a)  $U$  and (b)  $C$

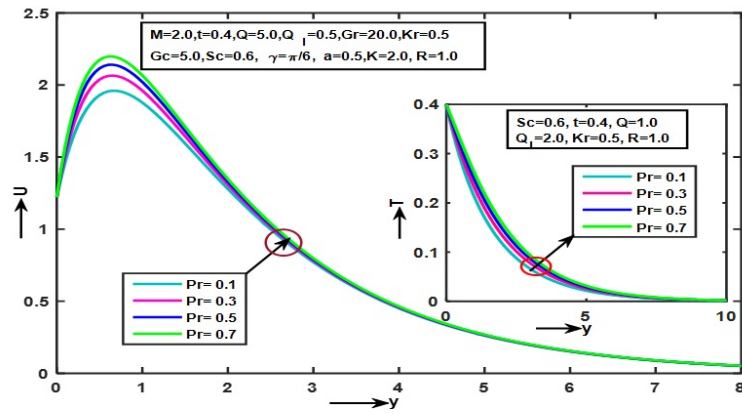


Figure 5.  $Pr$  impacts on  $U$  &  $T$ .

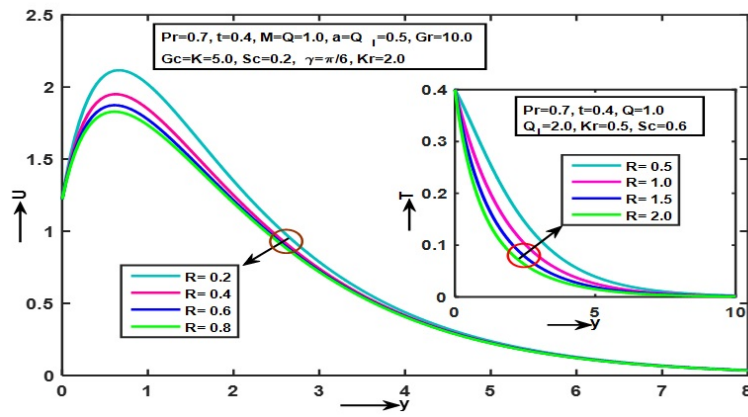


Figure 6.  $R$  impacts on  $U$  &  $T$ .

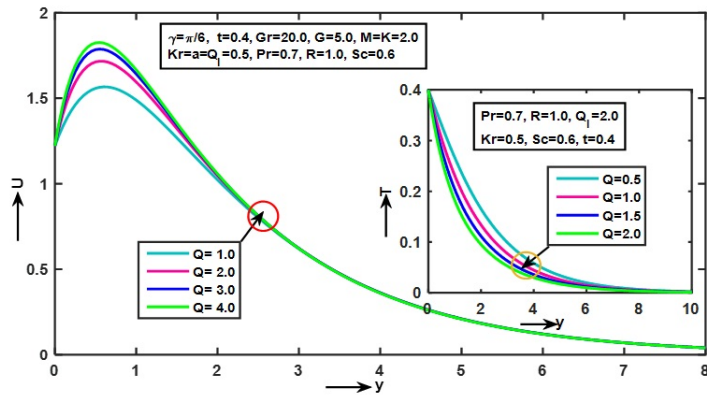


Figure 7.  $Q$  impacts on  $U$  &  $T$ .

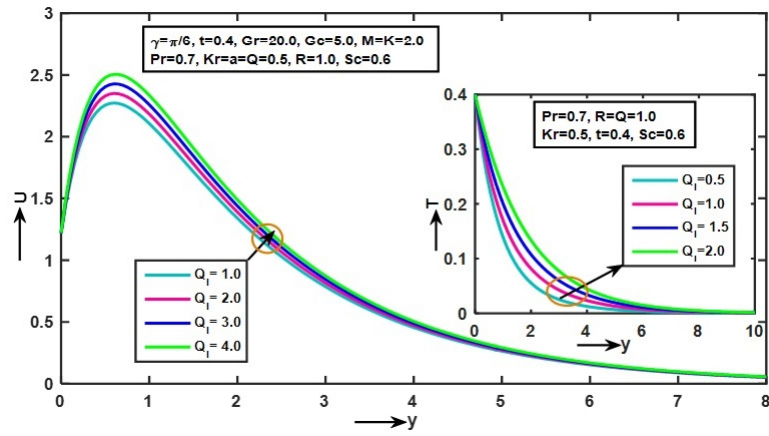
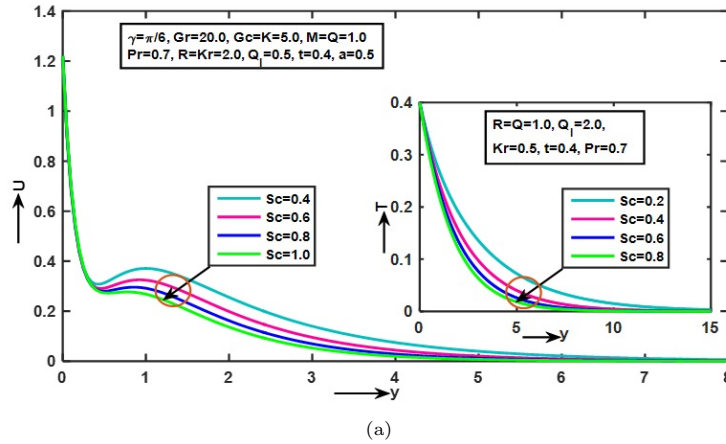
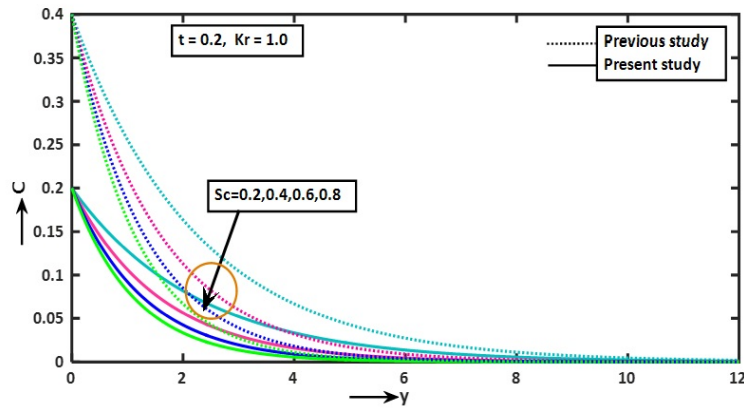


Figure 8.  $Q_l$  impacts on  $U$  &  $T$ .



(a)



(b)

Figure 9.  $Sc$  impacts on (a)  $U$ ,  $T$  and (b)  $C$

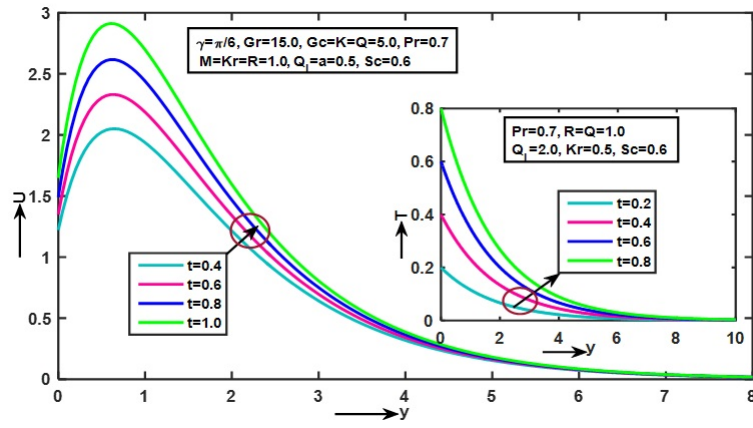
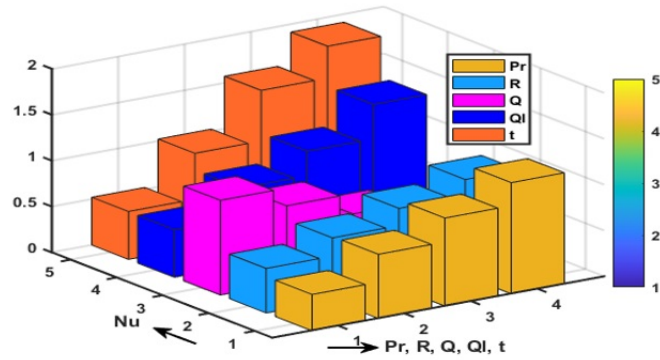
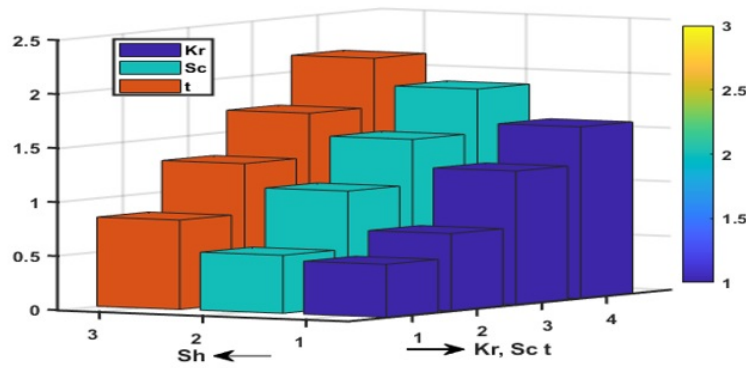


Figure 10.  $t$  impacts on  $U&T$ .



(a)



(b)

Figure 11. (a)  $Nu$  & (b)  $Sh$  Variations

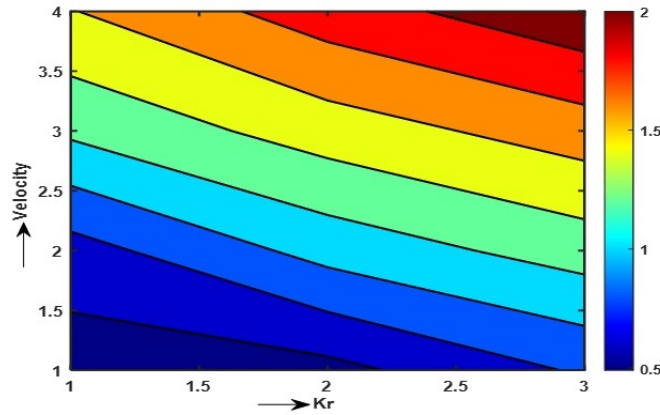


Figure 12. Velocity Contour

when the heat generation coefficient ( $Q > 0$ ) and the buoyancy force increase, which actuate the steam rate to increment. Fig.8 depicts the effects of different variations of the absorption quantity ( $Q_l$ ) on the velocity and temperature profiles. It is found that an increase in radiation absorption ( $Q_l$ ), the temperature and velocity enlarges the amount of heat in the liquid, which upsurges the warm and force limit layer width. Ultimately, the liquid hotness and speed expanded with the impact of heat generation and retention.

The effects on the concentration, hotness, and speed fields are illustrated in Figs. 9(a) & (b). It means that as pressure  $Sc$  increases, the concentration, temperature, and speed decrease. Additionally, the increase in atomic diffusivity and the outcome in the concentration limit layer diminishes, and then the species concentration is reciprocal to the smaller and higher values of  $Sc$ . The time on the liquid's hotness and speed is shown in Fig. 10. It is seen that both the profiles rise with the rising of time.

Fig.11(a) shows the Nusselt number variation for distinct values of  $Pr$ ,  $R$ ,  $Q$  and  $Q_l$ . It is obvious that the  $Nu$  rises as  $Pr$ ,  $R$ ,  $Q_l$  grow, however, negative phenomena are seen for different values of  $Q$ . It is interesting to note in Fig.11 (b) that the values of the  $Sh$  increase with the increasing values of the  $Kr$  and  $Sc$ . Based on the velocity contour shown in Fig.12 for various reaction values.

## 6. Conclusion

- The liquid velocity increases as Grashof, modified Grashof numbers, and permeability increase; however, the velocity decreases as the magnetic field spreads.
- The speed of the chemical reaction increased as it expanded, whereas the concentration decreased.
- Radiation absorption & Prandtl numbers create a noticeable expansion in the speed and heat.
- With an accelerated radiation and heat source, the speed and heat have a reciprocal relationship.

- As a result, Schmidt number, the concentration, hotness, and speed diminish.
- The resistance quantum magnifies with the rise of the magnetic field, but the rate of heat movement is de-escalated in more radiation and reaction as well as Schmidt number.

**Table 4.** Nomenclatures

$a$ : acceleration parameter	$R$ : radiation parameter
$B_0$ : magnetic field strength	$Sc$ : Schmidt number
$C'$ : fluid species concentration	$Sh$ : Sherwood number
$C'_w$ : fluid concentration at the plate	$T'_w$ : fluid temperature away from the plate
$C'_\infty$ : fluid concentration away from the plate	$T'_\infty$ : fluid temperature at the plate
$C_p$ : specific heat at constant pressure	$T'$ fluid temperature
$C_f$ : skin friction coefficient	$t'$ : time
$D$ : molecular diffusivity	$u'$ : fluid velocity in the $x'$ - direction
$Gc$ : modified Grashoff number	$u_0$ : plate velocity
$Gr$ : Grashoff number	$U$ : fluid velocity
$g$ : acceleration due to gravity	<b>Greek Symbols</b>
$K$ : porous permeability parameter	$\beta$ : volume expansion coefficient
$Kr$ chemical reaction parameter	$\beta'$ : thermal expansion coefficient
$M$ : magnetic field	$k$ : fluid thermal conductivity
$Nu$ : Nusselt number	$\sigma$ : fluid electrical conductivity
$Pr$ : Prandtl number	$\nu$ : kinematic viscosity
$Q$ : heat source parameter	$\rho$ : fluid density
$Q_t$ : radiation absorption parameter	$\mu$ : fluid viscosity
$q$ : heat flux	$\gamma$ : angle inclination

## 7. Funding

The authors received no monetary compensation for their research, authorship, or publication of this article.

## 8. Conflicts of interests/Competing interests

The authors have declared that there is no potential conflict of interest in the research, authorship, or publication of this article.

## 9. Data availability

This article's discussion of data sharing is not applicable because no datasets were created or examined for this particular investigation.

## References

- [1] S. Husain, Md. Adil, M. Arqam and B. Shabni, *A review on the thermal performance of natural convection in vertical annulus and its applications*, Renewable and Sustainable Energy Reviews, 2021, 150, 111463.
- [2] Siddartha, S. Rath, S.K. Dash, *Thermal performance of a wavy annular finned horizontal cylinder in natural convection for electronic cooling applications*, International Communications in Heat and Mass Transfer, 2021, 128, 105623.
- [3] K. Roy, A. Giri and B. Das, *A computational study on natural convection heat transfer from an inclined plate finned channel*, Applied Thermal Engineering, 2019, 159, 113941.
- [4] A. Abderrahmane, M. Hatami, M.A. Medebber, S. Haroun, S.E. Ahmed and S. Mohammed, *Non-Newtonian nanofluid natural convective heat transfer in an inclined half-annulus porous enclosure using FEM*, Alexandria Engineering Journal, 2021.
- [5] S.E. Ahmed, *Caputo fractional convective flow in an inclined wavy vented cavity filled with a porous medium using Al<sub>2</sub>O<sub>3</sub>-Cu hybrid nanofluids*, International Communications in Heat and Mass Transfer, 2020, 116, 104690.
- [6] Q. Khan, M. Farooq and S. Ahmad, *Convective features of squeezing flow in nonlinear stratified fluid with inclined rheology*, International Communications in Heat and Mass Transfer, 2021, 120, 104958.
- [7] D. Kumar and B.P. Chandran, *Investigation of transition in a natural convection flow in an inclined parallel plate channel*, International Communications in Heat and Mass Transfer, 2022, 130, 105768.
- [8] D. Yang, S. Ullah, M. Tanveer, S. Farid, M.I. Ur. Rehman, N.A. Shah and D. Chung, *Thermal transport of natural convection flow of second grade bio-nanofluid in a vertical channel*, Case Studies in Thermal Engineering, 2021, 28, 101377.
- [9] A.A. Zafar, J. Awrejcewicz, G. Kudra, N.A. Shah and S.J. Yook, *Magneto-free convection flow of a rate type fluid over an inclined plate with heat and mass transfer*, Case Studies in Thermal Engineering, 2021, 101249.
- [10] B.P. Geridomez and H.F. Oztop, *MHD natural convection in a cavity in the presence of cross partial magnetic fields and Al<sub>2</sub>O<sub>3</sub>-water nanofluid*, Computers & Mathematics with Applications, 2020, 80(12), 2796–2810.
- [11] M.M. Ali, R. Akhter and Md.A Alim, *Magneto-mixed convection in a lid driven partially heated cavity equipped with nanofluid and rotating flat plate*, Alexandria Engineering Journal, 2022, 61(1), 257–278.
- [12] N.C. Roy, *MHD natural convection of a hybrid nanofluid in an enclosure with multiple heat sources*, Alexandria Engineering Journal, 2022, 61(2), 1679–1694.
- [13] R. Khademi, A. Razminia and V.I. Shiryayev, *Conjugate-mixed convection of nanofluid flow over an inclined flat plate in porous media*, Applied Mathematics and Computation, 2020, 366, 124761.
- [14] G.A. Danish, M. Imran, M. Tahir, H. Waqas, M.I. Asjad, A. Ali and D. Baleanu, *Effects of nonlinear thermal radiation and chemical reaction on time*



- dependent flow of Williamson nanofluid with combine electrical MHD and activation energy*, Journal of Applied Computational Mechanics, 2021, 7(2), 546–558.
- [15] M.T. Akolade, A.T. Adeosun, and J.O. Olabode, *Influence of thermophysical features on MHD squeezed flow of dissipative Casson fluid with chemical and radiative effects*, Journal of Applied Computational Mechanics, 2021, 7(4), 1999–2009.
- [16] A. Tassaddiq, *MHD flow of a fractional second grad fluid over an inclined heated plate*, Chaos, Solitons & Fractals, 2019, 123, 341–346.
- [17] M.V. Krishna and A.J. Chamkha, *Hall and ion slip effects on MHD rotating flow of elastic-viscous fluid through porous medium*, International Communications in Heat and Mass Transfer, 2020, 113, 104494.
- [18] P. Mondal, T.R. Mahapatra and R. Parveen, *Entropy generation in nanofluid flow due to double diffusive MHD mixed convection*, Heliyon, 2021, 7(3), e06143.
- [19] H.K. Hamzah, F.H. Ali, M. Hatami and D. Jing, *Effect of two baffles on MHD natural convection in U-shape superposed by solid nanoparticle having different shapes*, Journal of Applied Computational Mechanics, 2020, 6(SI), 1200–1209.
- [20] N.S.S. Kumar, M. Madhu, S. Sindhu, B.J. Gireesha and N. Kishan, *Thermal analysis of MHD Williamson fluid flow through a microchannel*, International Communications in Heat and Mass Transfer, 2021, 127, 105582.
- [21] Hashim, A. Hamid and M. Khan, *Multiple solutions for MHD transient flow of Williamson nanofluids with convective heat transport*, Journal of the Taiwan Institute of Chemical Engineers, 2019, 103, 126–137.
- [22] B. Venkateswarlu and P.V. Satya Narayana, *Variable wall concentration and slip effects on MHD nanofluid flow past a porous vertical plate*, Journal of Nanofluids, 2019, 8(4), 838–844.
- [23] B. Venkateswarlu and P.V. Satya Narayana, *Cu-Al<sub>2</sub>O<sub>3</sub>/H<sub>2</sub>O hybrid nanofluid flow past a porous stretching sheet due to temperature dependent viscosity and viscous dissipation*, Heat Transfer, 2021, 50(1), 432–449.
- [24] P.V. Satya Narayana, B. Venkateswarlu and S. Venkataramana, *Thermal radiation and heat source effects on a MHD nanofluid past a vertical plate in a rotating system with porous medium*, Heat Transfer Asian Research, 2015, 44(1), 1–19.
- [25] A. Abbas, I. Ijaz, M. Ashraf and H. Ahmad, *Combined effects of variable density and thermal radiation on MHD Sakiadis flow*, Case Studies in Thermal Engineering, 2021, 28, 101640.
- [26] N.C. Roy, L.K. Saha and S. Siddiqua, *Electrohydrodynamics and thermal radiation effects on natural convection flow in an enclosed domain*, International Communications in Heat and Mass Transfer, 2021, 126, 105437.
- [27] P.J. Rani, G.C. Dash and S. Singh, *Radiation and mass transfer effects on MHD flow through porous medium past an exponentially accelerated inclined plate with variable temperature*, Ain Shams Engineering Journal, 2017, 8, 67–75.
- [28] M. Khan, A. Hafeez and J. Ahmed, *Impacts of non-linear radiation and activation energy on the axisymmetric rotating flow of Oldroyd-B fluid*, Physica A: Statistical Mechanics and its Applications, 2021, 580, 124085.

- [29] A. Hafeez, M. Khan and J. Ahmed, *Stagnation point flow of radiative Oldroyd-B nanofluid over a rotating disk*, Computer Methods and Programs in Biomedicine, 2020, 191, 105342.
- [30] B.K. Swain, *Effect of second order chemical reaction on MHD free convective radiating flow over an impulsively started vertical plate*, Journal of Nonlinear Modeling and Analysis, 3(2), 2021: 167–178.
- [31] A. Hafeez and M. Khan, *Flow of Oldroyd-B fluid caused by a rotating disk featuring the Cattaneo-Christove theory with heat generation/absorption*, International Communications in Heat and Mass Transfer, 2021, 123, 105179.
- [32] A. Hafeez, M. Khan, A. Ahmed and J. Ahmed, *Features of Cattaneo-Cgrustiv double diffusion theory on the flow of non-Newtonian Oldroyd-B nanofluid with Joule heating*, Applied Nanoscience, 2021.
- [33] A. Hafeez, M. Khan and J. Ahmed, *Thermal aspects of chemically reactive Oldroyd-B fluid flow over a rotating disk with Cattaneo-Christove heat flux theory*, Journal of Thermal Analysis and Calorimetry, 2020.
- [34] P.M. Raju, S.S. Reddy and M.N. Shekar, *Transient MHD flows through an exponentially accelerated isothermal vertical plate with Hall effect and chemical reaction*, Partial Differential Equations in Applied Mathematics, 2021, 4, 100047.
- [35] . K. Sing, A.K. Pandey and M. Kumar, *Slip flow of micropolar fluid through a permeable wedge due to the effects of chemical reaction and heat source/sink with Hall and iso-slip currents: an analytic approach*, Propulsion and Power Research, 2020, 9(3), 289–303.
- [36] . P.V. Satya Narayana, B. Venkateswarlu and S. Venkataramana, *Chemical reaction and Radiation absorption effects on MHD micropolar fluid past a vertical porous plate in a rotating system*, Journal of Energy Heat and Mass Transfer, 2013, 35(3), 197–214.
- [37] . P.V. Satya Narayana, B. Venkateswarlu and S. Venkataramana, *Effects of Hall current and radiation absorption on MHD micropolar fluid in a rotating system*, Ain Shams Engineering Journal, 2013, 4(4), 843–854.
- [38] K. Das, *Slip effects on heat and mass transfer in MHD micropolar fluid flow over an inclined plate with thermal radiation and chemical reaction*, International Journal for Numerical Methods in Fluids, 2012, 70(1).
- [39] X. Qiang, I. Siddique, K. Sadiq and N.A. Shah, *Double diffusive MHD convective flows of a viscous fluid under influence of the inclined magnetic field, source/sink and chemical reaction*, Alexandria Engineering Journal, 2020, 59 (6), 4171–4181.
- [40] S. Ahmad, A. Ahmad, K. Ali, H. Bashir and M.F. Iqbal, *Effect of non-Newtonian flow due to thermally-dependent properties over an inclined surface in the presence of chemical reaction, Brownian motion and thermophoresis*, Alexandria Engineering Journal, 2021, 60(5), 4931–4945.
- [41] N. Imran, M. Javed, M. Sohail, P. Thounthong and Z. Abdelmalek, *Theoretical exploration of thermal transportation with chemical reactions for scutterby fluid model obeying peristaltic mechanism*, Journal of Materials Research and Technology, 2020, 9(4), 7449–7459.

- 
- [42] A.G.K. Kumar and S.V.K. Varma, *Radiation effects on MHD flow past an impulsively stated exponentially accelerated vertical plate with variable temperature in the presence of heat generation*, International Journal of Engineering Science and Technology, 2011, 3(4), 2897–2909.
- [43] D. Harish Babu, K.A. Ajmath, B. Venkateswarlu and P.V. Satya Narayana, *Thermal radiation and heat source effects on MHD non-Newtonian nanofluid flow over a stretching sheet*, Journal of Nanofluids, 2018, 8(5), 1085–1092.
- [44] B. Venkateswarlu, K. Bhagya Lakshmi, S. Samantha Kumari and P.V. Satya Narayan, *Magnetohydrodynamic oscillatory flow of a physiological fluid in an irregular channel*, SA Applied Sciences, 2019, 1(10), 1–13.